



Title	The effects of extrinsic factors on the structural and mechanical properties of <i>Pseudomonas fluorescens</i> biofilms: A combined study of nutrient concentrations and shear conditions
Authors(s)	Allen, Ashley, Habimana, Olivier, Casey, Eoin
Publication date	2018-05-01
Publication information	Allen, Ashley, Olivier Habimana, and Eoin Casey. "The Effects of Extrinsic Factors on the Structural and Mechanical Properties of <i>Pseudomonas Fluorescens</i> Biofilms: A Combined Study of Nutrient Concentrations and Shear Conditions" 165 (May 1, 2018).
Publisher	Elsevier
Item record/more information	http://hdl.handle.net/10197/24160
Publisher's statement	This is the author's version of a work that was accepted for publication in <i>Colloids and Surfaces B: Biointerfaces</i> . Changes resulting from the publishing process, such as peer review, editing, corrections, structural formatting, and other quality control mechanisms may not be reflected in this document. Changes may have been made to this work since it was submitted for publication. A definitive version was subsequently published in <i>Colloids and Surfaces B: Biointerfaces</i> (VOL 165, (2018)) DOI: https://doi.org/10.1016/j.colsurfb.2018.02.035
Publisher's version (DOI)	10.1016/j.colsurfb.2018.02.035

Downloaded 2023-10-31T04:02:18Z

The UCD community has made this article openly available. Please share how this access benefits you. Your story matters! (@ucd_oa)



© Some rights reserved. For more information

1 The effects of extrinsic factors on the structural and
2 mechanical properties of *Pseudomonas fluorescens* biofilms:
3 the combined study of nutrient concentrations and shear
4 conditions

5

6 Ashley Allen^a, Olivier Habimana^b, Eoin Casey^{c*}

7

8 ^a School of Engineering, The University of Edinburgh, Edinburgh, UK

9 ^b School of Biological Sciences, The University of Hong Kong, Pokfulam, Hong Kong, SAR,
10 People's Republic of China.

11 ^c School of Chemical and Bioprocess Engineering, University College Dublin (UCD), Belfield,
12 Dublin 4, IRELAND

13 *Corresponding author: Phone: +353 1 716 1877, Email: eoin.casey@ucd.ie

14 Number of words in manuscript: 6260 (including references)

15 Number of Tables: 2

16 Number of Figures: 4

17 **ABSTRACT**

18 The growth of biofilms on surfaces is a complicated process influenced by several
19 environmental factors such as nutrient availability and fluid shear. In this study, combinations
20 of growth conditions were selected for the study of *Pseudomonas fluorescens* biofilms
21 including as cultivation time (24- or 48 hours), nutrient levels (1:1 or 1:10 King B medium),
22 and shear conditions (75 RPM shaking, 0.4 mL min⁻¹ or 0.7 mL min⁻¹). The use of Confocal
23 Laser Scanning Microscopy (CLSM) determined biofilm structure, while liquid-phase Atomic
24 Force Microscopy (AFM) techniques resolved the mechanical properties of biofilms. Under
25 semi-static conditions, high nutrient environments led to more abundant biofilms with three
26 times higher EPS content compared to biofilms grown under low nutrient conditions. AFM
27 results revealed that biofilms formed under these conditions were less stiff, as shown by their
28 Young's modulus values of 2.35 ± 0.08 kPa, compared to 4.98 ± 0.02 kPa for that of biofilms
29 formed under high nutrient conditions. Under dynamic conditions, however, biofilms exposed
30 to low nutrient conditions and high shear rates led to more developed biofilms compared to
31 other tested dynamic conditions. These biofilms were also found to be significantly more
32 adhesive compared to their counterparts grown at higher nutrient conditions.

33

34 **KEYWORDS:** *Pseudomonas fluorescens*, biofilm, nutrient concentration, shear, Confocal
35 laser scanning microscopy, Atomic force microscopy, biofilm viscoelastic properties.

36

37 **1. INTRODUCTION**

38 Biofilms are an aggregation of bacteria attached to a surface and embedded in a protective
39 matrix. This protective matrix consists of layers of extracellular polymeric substances (EPS)
40 surrounding the bacteria and comprises a variety of macromolecules, polysaccharides, proteins,

41 DNA, nucleic acids, enzymes, lipopolysaccharides and phospholipids among other substances
42 [1]. The physical stability of this matrix is dependent on weak-physicochemical interactions.
43 An increase in multi-valent ionic agents such as CaCl_2 or AlCl_3 may provide strong
44 crosslinking replacing any hydrogen bonding within the EPS matrix, and can result in higher
45 mechanical stability of the biofilm structure [2, 3]. The modulatory properties of supplemented
46 CaCl_2 have also been shown to influence the structural and mechanical properties of *P.*
47 *fluorescens* biofilms by lowering stiffness and increasing adhesiveness [4]. More recently, the
48 effects of CaCl_2 on *P. fluorescens* biofilm mechanical properties were validated using a
49 particle-tracking micro-rheology method [5]. The response to CaCl_2 may nonetheless result in
50 different outcomes depending on the microbial species within the biofilm. For example,
51 Flemming et al. [1] noted that *Pseudomonas aeruginosa*, grown in the presence of CaCl_2
52 produced a thick, compact and mechanically stable biofilm. These differences in biofilm
53 properties were attributed to the interaction of Ca^{2+} ions between polyanionic alginate
54 molecules. In a similar study involving *Pseudomonas aeruginosa* grown at an air-liquid
55 interface, Abraham et al. demonstrated that the addition of either monovalent or divalent salts
56 was sufficient to cause a distinct compact structural biofilm phenotype [6]. The presence of
57 ionic agents is, therefore, known to influence biofilm structural and mechanical properties.
58 However, other factors such as nutrient concentration and shear conditions may also be
59 considered as extrinsic factors, hence requiring further investigation.

60 Such factors cannot be ignored, especially in many industrial sectors (i.e. food and
61 water processing industries), known for providing ideal environments for the growth and
62 proliferation of unwanted biofilms. Most notably, the adhesive nature of biofilms is responsible
63 for the high operational costs associated with cleaning procedures, equipment damage or
64 replacements, and process losses. Irrespective of where they are found, biofilm development

65 will depend on some extrinsic factors that may affect its growth, of these, nutrient availability
66 and shear force.

67 The effects of nutrient concentration have been demonstrated to influence bacterial
68 adhesion [7, 8]. Peyton et al. (1996) using *P. aeruginosa* showed that a higher substrate loading
69 rate led to increased biofilm thickness, roughness and areal mass density [9]. In a separate
70 study, Moreira et al. (2015) also demonstrated that biofilm characteristics were influenced by
71 different surface properties, agitation and nutrient concentration [10].

72 Biofilms can form under a range of hydrodynamic conditions, and the fluid shear stress
73 is known to influence biofilm thickness and structure [11, 12]. For example, under laminar
74 flow, roughly circular micro-colonies were found to be separated by water channels, whereas
75 in turbulent flow, filamentous streamers can form with ripple-like structures after continued
76 growth [13]. In general, biofilms cultivated under turbulent flow conditions display stable and
77 rigid structures, whereas laminar flow leads to thicker but less dense biofilms [12, 14]. Studies
78 by Moreira et al. demonstrated that under high shear conditions, *E. coli* biofilms were still able
79 to develop under low glucose concentrations as low as 0.25 gL^{-1} for 12 hours [15]. In a shear
80 stress stimulation study, Horn et al. noted that biofilm detachment only occurred once a certain
81 biofilm-thickness is reached [16]. Nevertheless, little is known of the changes in adhesive and
82 elastic properties of the biofilms grown under shear stress under semi-static and dynamic
83 conditions, thereby justifying the need for further quantification of the biofilm material
84 properties under such conditions.

85 Nanoindentation, through Atomic Force Spectroscopy, has advanced into a technique
86 capable of providing adhesive and cohesive forces of both single cells and biofilm aggregates
87 [4, 17]. The Hertz model [18] has been successfully employed in nanoindentation experiments
88 to estimate the elastic modulus of the surface indented [19, 20]. This well-established model
89 provides an estimate of the elastic modulus from the area of non-adhesive contact of an

90 indentation curve. The analysis of the retraction section of indentation curves revealed the
91 adhesive properties of the material. The adhesive property is an indicator of the level of EPS
92 produced by the biofilm [21, 22]. As demonstrated in an earlier study using AFM, EPS levels
93 could be quantified by comparing interaction forces between sulphate reducing bacteria and
94 cantilever tips, by determining the differences in elastic forces [23]. While the study by Fang
95 et al. assesses the EPS production in various areas of a single cell, the present study employed
96 a previously described experimental approach used by Safari et al., in which biofilm EPS is
97 quantified utilising a combination of Con A staining with advanced microscopy [4].

98 The objective of this study was to investigate the effects of nutrient concentration on the
99 mechanical and structural formation of 24-hour grown *Pseudomonas fluorescens* biofilm under
100 dynamic conditions. The adhesive and cohesive forces of the biofilm surface layer were
101 measured using a colloidal probe for nanoindentation experiments in liquid. Additionally, the
102 structural analysis was performed by confocal laser scanning microscopy (CLSM) with biofilm
103 staining for the differentiation between bacterial cells and EPS biofilm fractions.

104

105 2. METHODS

106 2.1. Bacterial strains, cultural conditions and preparation

107 The mCherry expressing *Pseudomonas fluorescens* PCL 1701 [24] was selected for the biofilm
108 adhesion assays. *P. fluorescens* was stored at -80 °C in King B [25] broth supplemented with
109 20 % glycerol. Cultures were obtained by selecting a single colony grown on King B agar
110 (Sigma Aldrich, Ireland) at 28 °C and inoculating 100 mL King B broth supplemented at a final
111 concentration of 10 µg mL⁻¹ of gentamicin (Sigma Aldrich, Ireland). The inoculation medium
112 was then incubated at 28 °C with shaking at 75 rpm for 16 hours until an optical density (OD)
113 of 0.8-1.0 at a wavelength of 600 nm was obtained. Cultures were centrifuged at approximately

114 4000g (Eppendorf Centrifuge 5415C, Rotor F-45-18-11) for 10 min. Subsequently, the
115 supernatant was discarded, and the bacterial pellet was re-suspended in sterile King B.

116

117 2.2. Biofilm growth with different nutrient concentrations

118 A semi-static biofilm was grown as described by Ashkan et al. [4]. To ensure sterility centrifuge
119 tubes (Falcon, Fisher Scientific, Ireland) containing coverslips of Borosilicate Glass 22 mm ×
120 22 mm (VWR, Ireland) were sealed with cotton wool and autoclaved. 3 mL of King B of at
121 selected concentrations were subsequently inserted into the sterile centrifuge tubes. One tube
122 contained 100 % King B (dilution factor of 1:1) while a second tube consists of 10 % King B
123 and 90% Grade 1 pure water (dilution factor of 1:10), referred to as MilliQ water (Biopure 15
124 and Purelab flex 2, Veolia, Ireland). The 3 mL of the medium was supplemented with
125 gentamicin (Sigma Aldrich, Ireland) at a final concentration of 10 µg mL⁻¹. Each tube was
126 inoculated with a 5 µl volume of the re-suspended overnight culture. Centrifuge tubes were
127 incubated over a period of 24 hours, with an orbital agitation of 75 rpm and temperature of 28
128 °C.

129

130 2.3. Dynamic Biofilm Growth

131 Flow cell systems allow for the direct measurement of biofilm using direct microscopic
132 observation. The flow cells used were model BST 81 from Biosurface Technologies
133 Corporation (Bozeman, MT, USA). This flow cell was used to examine the 48-hour growth of
134 *P. fluorescens* biofilm on a coverslip using different nutrient concentrations. King B was
135 prepared in a 20 L feed tank at two different dilution factors of 1:1 (high nutrient) and 1:10
136 (low nutrient). To ensure sterility, the flow cell system, with the exception the waste tank, was
137 autoclaved. The flow cell system was placed in an oven at 28 °C and left for one hour to allow
138 the feed tank (ThermoFisher, UK) temperature to achieve equilibrate. The pH was checked
139 using a Mettler Toledo pH-meter (Mason Laboratories, Dublin) at both the three-way valve

140 and the waste tank using a 50 mL tube. The system was maintained at a pH of 7.4 until bacterial
141 injection. Biofilm within the flow cell chamber was grown by injecting 5 mL *P. fluorescens*
142 into the three-way valve (Cole-Parmer, IL, USA). The bacterial cells were then temporarily
143 allowed to settle onto the coverslip for 1 hour under static conditions without flow. The flow
144 of the liquid through the chamber was controlled by pumping media through the silicone tubing
145 (VWR, Ireland) into the flow chamber. A continuous flow of media through the flow cell
146 chamber was maintained by a Watson-Marlow 205S peristaltic pump (OH, USA). After 48
147 hours the King B media was replaced with a flow of PBS that was injected into the flow cell
148 system using the 3-way valve for 15 minutes. The valves on both ends of the flow cell were
149 closed, and the flow cell was disconnected from the system at the point where these valves had
150 been closed. Two different flow rates were used, one at 0.4 mL min⁻¹ and 0.7 mL min⁻¹
151 corresponding to a Re_{dh} of 0.42 and 0.85 respectively. The flow cell was then analysed by
152 confocal laser scanning microscopy using a custom-made holder.

153

154 2.4. Confocal Laser Scanning Microscopy and staining

155 Coverslips were removed from the centrifuge tubes and gently washed with a sterile 0.1 M
156 NaCl solution. For bacterial and EPS staining Syto 9[®] (green nucleic acid stain: Molecular
157 Probes) and Concanavalin A (Con A) staining protocol in conjunction with a fluorophore
158 (Alexa Fluor 633) (Life Technologies™) was employed. Post rinsing the biofilms are stained
159 with Syto 9[®] at a final concentration of 3.5 µg ml⁻¹. Stained biofilms were rinsed with a sterile
160 0.1M NaCl solution and subsequently stained with Con A-AlexaFluor633 at a final
161 concentration of 200 µg ml⁻¹. Finally, the coverslip is rinsed preceding confocal microscopy.

162 The coverslips were placed in a phosphate buffered saline (PBS) solution (Sigma
163 Aldrich, Ireland) enclosed by a Nunc Lab-Tek II Chamber Slide (VWR, Ireland). Confocal
164 Laser Scanning Microscopy was performed using an Olympus FV1000 CLSM at the Live Cell

165 Imaging core technology facility platform, Conway Institute, UCD. Experiments were repeated
166 to provide biofilms from 3 independent inocula for both growth conditions resulting in up to 3
167 different areas of 3 biofilms, these were repeated for both stained and unstained biofilms.
168 The two wavelengths were used for EPS and bacterial analysis Syto 9[®] and Con A-
169 AlexaFluor633, excited at 488 nm and 633 nm respectively. 3D projections were collected at
170 a z-step of 1 μm using an Olympus UPL SAPO 10 \times / 0.4 NA air objective. The biofilms
171 structural quantification was performed using Image Structure Analyzer 2 [26, 27].
172 Quantification of coverage of EPS and bacteria for vertical distribution analysis was
173 implemented using Image J from NIH (<https://imagej.nih.gov/ij/>).

174

175 2.5. Cantilever Preparation and Atomic Force Microscopy Observations

176 Atomic Force Microscopy (AFM) was performed on biofilm to obtain the indentation and
177 retraction curves to determine the elastic and adhesive properties. These force measurements
178 were performed using an Asylum Research MFP-3D AFM (California, US) and Nikon Ti/E
179 fluorescence microscope (Nikon, Japan), which was placed on a vibration table and enclosed
180 in an acoustic isolation chamber (TS-150, JRS Scientific Instruments, Switzerland).

181 Cantilevers used in the experiments were created using a micromanipulator DC-3K
182 with a push button controller MS 314 (Märzhäuser Wetzlar GmbH & Co. KG, Germany). Small
183 amounts of UV curable epoxy resin (TE Connectivity Chemicals, USA) were placed on an
184 NSC 12 E tip-less cantilever (*MicroMasch*, Lithuania). 10 μm silica spheres MSS1-10
185 (Whitehouse Scientific, United Kingdom) were then attached to the epoxy on the surface of
186 the cantilever using a separate pipette. The colloidal probe was subsequently cured in an oven
187 at 100 $^{\circ}\text{C}$ for 1 hour. Usable probes were then imaged and calibrated using the thermal noise
188 method [28] as 0.13 N m^{-1} at room temperature.

189 Force curves were performed on biofilm at the air-liquid interface. Biofilms were rinsed in a
190 0.1 M NaCl solution and placed in the AFM holder. Experiments were performed in duplicate
191 for each biofilm condition, and biofilms remained in PBS solution during measurement. At
192 least 100 force curves measurements were obtained for each biofilm at a scan rate of $0.5 \mu\text{m}^{-1}$
193 and force set point limit of 8-10 nN. After each force map, the cantilever was tested on the
194 glass to ensure no biofilm residue had attached. If tip contamination had occurred the cantilever
195 was rinsed with ethanol then MilliQ water and placed in a UV ozone cleaner (ProCleaner,
196 Bioforce Nanosciences, Ames, IA) for 15 min.

197 Force Curves were analysed using the Hertz model fitting of Protein Folding and
198 Nanoindentation Software (PUNIAS, <http://punias.free.fr/>) [29] with the Poisson ratio taken as
199 a constant of 0.5.

200 2.6. Statistical Analysis

201 Data present are the mean \pm standard error of the mean. Statistical analysis was performed by
202 analysis of invariance (ANOVA) in Tukey's test for pairwise comparisons using MINITAB
203 v15.1 (Minitab Inc., State College, PA) at a level of significance of 5 % ($p < 0.05$).

204

205 3. RESULTS AND DISCUSSION

206 3.1. Qualitative analysis of biofilm grown under semi-static and dynamic
207 conditions

208 The influence of nutrient concentration levels and shear stress on the structure of *P. fluorescens*
209 biofilms was investigated during 24- to 48-hour assays. Shear stress was introduced during
210 both dynamic and semi-static biofilm assays, as shear is known to induce the erosion and
211 sloughing of biofilms during their development [30]. Under semi-static growth conditions,
212 biofilms were allowed to develop at the air-liquid interface areas. Shear was introduced in the

213 form of capillary forces as the tube reactor was gently shaken during the assay. Under dynamic
214 conditions, using a flow cell, higher shear conditions could be obtained by adjusting flow rates
215 conditions, to 0.4 mL min⁻¹ or 0.7 mL min⁻¹.

216 Three-dimensional reconstructions of *P. fluorescens* biofilms grown under semi-static
217 conditions at high nutrient (1:1) and low nutrient (1/10 diluted King B) levels are presented in
218 (Figure 1). Biofilms grown under high nutrient conditions (A) exhibited large heterogeneous
219 biofilm clusters with EPS (in red) covering most of the bacterial cells (green). Conversely,
220 biofilms grown under low nutrient conditions (B) were characterised as a homogenous
221 monolayer of smaller cell clusters, mostly consisting of bacterial cells (green).

222 Biofilms grown under high nutrient environments were found to be comparable to those
223 published previously under similar conditions [5]. Biofilms grown under lower nutrient
224 condition (Figure 1a) displayed a noticeably reduced biomass bulk. Several studies suggest that
225 nutrient limitation may influence the growth rate of the biofilm resulting in the reduction of
226 biofilm [31, 32],

227 Under dynamic conditions (Figure 2), the level of biofilm formation was linked to the
228 specific nutrient environments. High nutrient conditions (A-B) led to lower biofilm
229 development, as characterized by their heterogeneously spread cell clusters. Under lower
230 nutrient levels (C-D), biofilms grown at high flow rate led to fully developed homogenous flat
231 biofilms (C), compared to those grown at lower shear conditions characterised by its
232 heterogeneously spread cell clusters (D). The distribution profile of each biofilm was
233 additionally examined to gain a better understanding of the bacterial spatial distribution within
234 biofilms (Supplementary information, figure S1).

235 An incubation period of 48 hours for flow-cell biofilm growth was intended to allow
236 the bacteria to establish themselves on the glass surface under shear stress. These were
237 compared to 24-hour biofilms grown under semi-static conditions to assess growth pattern of

238 a 'mature' biofilm. From Figure 2, biofilm formation in low dynamic conditions produced a
239 greater volume of biofilm with higher surface coverage, which also agrees with Dewanti et al.
240 who studied the cell adhesion and biofilm formation of *E. coli* on stainless steel. The authors
241 showed that under dynamic conditions, biofilms in low nutrient media grew faster [33]. A
242 recently published article also supports this finding whereby, under certain conditions,
243 (specifically phosphorous limitation), EPS production was enhanced [34]. Similarly, it was
244 previously shown that the biofilm matrix may play a role in the sorption nutrients and minerals
245 from surrounding aqueous environment [35]. Patterson et al. noted that the initial adhering
246 bacteria play a vital role in the characteristics of the subsequent biofilm structure [36]. By
247 producing a greater volume of EPS under low nutrient environments in early stage biofilms,
248 there may be an increased biofilm development due to the enhanced sorption of nutrients.

249 3.2. Quantitative analysis of biofilms grown under semi-static conditions

250 Biofilms grown under semi-static conditions in either low or high nutrient environments were
251 quantified in term of total biovolume (μm^3), substratum coverage (%), mean thickness (μm)
252 and biofilm roughness derived from CLSM acquisition data (Table 1). The effects of nutrient
253 environments on biofilm development were characterised by staining biofilms with Syto 9[®]
254 nucleic acid total stain, while the effects on EPS production under tested nutrient growth
255 conditions were quantified using lectin-based EPS stain Concanavalin A (conA), as presented
256 in Table 1.

257 A two-fold difference in total cell biovolume was observed ($p = 0.004$) between biofilms grown
258 under high nutrient and low nutrient conditions with values of $56988 \pm 14379 \mu\text{m}^3$ and 27593
259 $\pm 4714 \mu\text{m}^3$ respectively. Growth under high nutrient conditions was also characterised by a
260 three-fold increase in EPS levels compared to biofilms grown under low nutrient conditions (p
261 $= 0.003$, as observed by their biovolume: $68453 \pm 12278 \mu\text{m}^3$ and $18463 \pm 3129 \mu\text{m}^3$
262 respectively. EPS production is known to assist in the growth and proliferation of embedded

263 cells within the biofilm [37, 38]. This threefold increase in EPS production may be largely
264 attributed to higher nutrient availability. Comparison of biofilm surface coverage values and
265 EPS levels at low nutrient conditions versus high nutrient conditions were found to be 1.6- and
266 2.2-fold higher respectively ($p = 0.026$ and $p = 0.007$). High nutrient conditions led to more
267 structured biofilms as observed by higher biofilm roughness values for both total cells and EPS
268 level, compared to biofilms grown under low nutrient conditions ($p = 0.018$ and $p = 0.003$
269 respectively). Mean biofilm thickness was not shown to be affected by nutrient growth
270 conditions ($p > 0.05$) and this may be as a result of the imposed shear.

271 As shown in a study by Nguyen et al., bacteria develop an antibiotic tolerance when starved
272 from nutrients. However, this results in the restriction of growth. For bacteria susceptible to
273 gentamicin the reduced nutritional strain may result in a reduction of biofilm growth and
274 proliferation instead opting for the production of EPS to protect and promote long-term biofilm
275 survival [39].

276 3.3. Quantitative analysis of biofilms grown under dynamic conditions

277 Quantitative analyses of 48-hour grown *P. fluorescens* biofilms under dynamic conditions were
278 also performed (Figure 3). Here, biofilms were grown under high and low nutrient conditions,
279 and at different flow rates of 0.4 mL min^{-1} (low flow rate) and 0.7 mL min^{-1} (high flow rate).

280 *P. fluorescens* biofilm grown for 48 hours under high nutrient conditions at high and low flow
281 rates show no significant difference in biovolume, substratum coverage, thickness or roughness
282 ($p > 0.05$). For biofilms grown at low nutrient conditions at both low and high flow rates, there
283 was no significant structural difference regarding biovolume, thickness and roughness ($p >$
284 0.05). A significant difference was however observed for substratum coverage ($p = 0.04$),
285 which was found to cover a 60% larger area under the high flow rate compared to low flow
286 rate condition. The lack of quantifiable differences in biofilm characteristics could have been

287 attributed to the selected flow rates (two-fold difference) conditions used in this study.
288 Nevertheless, this result also aligns with conclusions from previously published research [36]
289 where a four-fold difference in shear rate was used.

290 While no differences in structural biofilm parameters were observed based on flow rate
291 conditions or shear stress, the level of nutrient growth was shown to have affected biofilm
292 structure, irrespective of flow rate conditions. More specifically, low nutrient conditions led to
293 biofilms with 1.5 times and 2.5 higher total biovolume compared to biofilms formed under
294 higher nutrient environments at low ($p = 0.008$) and high ($p = 0.005$) flow rates respectively.
295 The same observation also applies to surface coverage, in which nutrient level during growth
296 rather than flow rate conditions led to generally thicker biofilms ($p < 0.05$). In contrast, the
297 nutrient level was not shown to have significantly affected biofilm roughness characteristics (p
298 $= 0.238$).

299 From these results, it can be determined that *P. fluorescens* biofilm growth was
300 influenced by changes in nutrient availability, particularly at low flow rates concerning
301 substratum coverage. This effect is prominent under low nutrient conditions whereby the
302 biofilm seems to produce EPS, to protect and absorb nutrients from the depleted environment,
303 thereby promoting biofilm survival.

304 3.4. Mechanical analysis of biofilms

305 The influence of nutrient concentration levels on the structure of 24-hour semi-static *P.*
306 *fluorescens* biofilms was investigated using Atomic Force Microscopy. The assessment of
307 biofilms grown under dynamic conditions was not conducted since the removal from flow cells
308 would result in noticeable biofilm disruption. Nanoindentation acquisitions were conducted on
309 biofilms that had developed at the air-liquid interface. All force curves were performed in PBS
310 with a set-point limit of 9-12 nN. Biofilm samples grown under high-nutrient conditions

311 displayed a substantial indentation depth ($0.20 \pm 0.08 \mu\text{m}$) when compared to biofilms under
312 low nutrient environments ($0.08 \pm 0.007 \mu\text{m}$). Moreover, the resulting indentation was less
313 than 10% of the overall biofilm depth measured by CLSM which is within the valid range for
314 the Hertz model. The differences in biofilm force-indentation curves indicate a stiffer biofilm
315 sample surface with low nutrient availability.

316 The Young's modulus of 24-hour *P. fluorescens* semi-static biofilms, grown under low-
317 and high-nutrient availability are presented in Figure 4. Biofilm development under low-
318 nutrient environments displayed a higher elastic modulus of $4.98 \pm 0.02 \text{ kPa}$ compared to the
319 lower elastic modulus of $2.35 \pm 0.08 \text{ kPa}$ under high-nutrient environments. Additionally, the
320 complete overlap of approach and retraction curve during nanoindentation may not occur as
321 the biofilm can display a limited degree of plastic deformation [40] which may result in higher
322 elastic values. Nevertheless, the results show that under low nutrient growth conditions, the
323 biofilms were twice as stiff as those grown under high nutrient conditions. The elastic modulus
324 is higher than reported by Zeng et al. who conducted nanoindentation on *P. fluorescens* biofilm
325 using a $59.2 \mu\text{m}$ colloid cantilever, which resulted in a Youngs modulus of $0.10 \pm 0.01 \text{ kPa}$
326 [40]. However, the biofilm cultivation conditions most likely result in the various between
327 Youngs modulus values.

328 Greater EPS was produced in biofilms developing under high-nutrient environments,
329 resulting in a significant elastic response, as defined by high biofilm viscosity. EPS production
330 significantly altered the physical structure of the cell-substrate interface, resulting in a softer
331 biofilm. In contrast, stiffer biofilm properties, as characterized by the higher elastic modulus,
332 was observed for biofilms grown under low nutrient environments. The observed biofilm
333 stiffness may be associated with lower levels of produced EPS, compounded by bacterial
334 monolayers of single cells at the surface during nanoindentation. Safari et al. noted that *P.*
335 *fluorescens* biofilm with the addition of calcium ions produced higher EPS sugar residues

336 following 48-hour biofilms growth under semi-static conditions. The observed differences in
337 biofilm formation suggest specific bacterial response depending on nutrient availability and
338 specific composition. Steinberger et al. observed *Pseudomonas aeruginosa* cells, grown on
339 membranes for 16 hours in static conditions, elongated while a constant width was maintained
340 under lower nutrient conditions. They suggested this elongation resulted in an improvement in
341 the collection of nutrients from the feed source, without changes in the ratio of surface to
342 volume [41]. In the present study, the low nutrient-induced elongation of bacteria may have
343 led to a higher elastic modulus by directly indenting on bacterial cells rather than on an EPS
344 layer covering the cells.

345 The average adhesive force and work of adhesion of 24-hour *P. fluorescens* biofilms
346 grown under static conditions at low- and high-nutrient environments are shown in Table 2.
347 Biofilms grown under low nutrient environments were shown to have a stickier surface with a
348 7-fold increase in the adhesive force ($p < 0.001$). Compared to high-nutrient environments,
349 biofilms developing under low nutrient conditions seem to have produced a hard and sticky
350 biofilm surface, as determined by its characteristic higher work of adhesion compared to
351 biofilm grown under high nutrient conditions ($p < 0.001$) (Figure 4). In principle, an increase
352 in adhesion energy is typically associated with greater attachment of the substrate to the
353 cantilever tip and may indicate an increased volume of EPS [4, 42, 43]. This difference in
354 adhesion forces is suggested to occur due to a stronger stretching of polyproteins [44].
355 However, the higher stiffness may be due to nanoindentation occurring on a thin layer of EPS
356 covering the cells within the biofilm.

357 It has been shown the EPS of different microorganisms might vary in their mechanical
358 properties such as stickiness and viscosity and that this EPS accumulation can result in a
359 variation in the measurement of elasticity [45, 46]. Nutrients, however, may also play an
360 essential role in the production of EPS during biofilm growth, consequently influencing the

361 biofilm's viscoelastic and adhesive character [47]. Francius et al. researched the EPS coverage
362 of *Lactobacillus rhamnosus GG* cells. By comparing wild-type and mutant strains with limited
363 EPS production, they determined that the cells were covered in a smooth, ridge lattice of
364 globular proteins, the roughness of which was on the nanometer scales, whereas the
365 polysaccharide producing cells were rougher [48]. As biofilms under low nutrient conditions
366 produced lesser EPS than under high nutrient conditions, the cantilever may be directly
367 interacting with cell wall globular proteins, thereby resulting in the observed higher adhesive
368 forces.

369 Other properties to consider when discussing adhesive forces of the biofilm is the
370 physicochemical and mechanical properties of the colloid cantilever used during acquisition.
371 Surface roughness has been shown to influence the adhesion of bacteria to the surface [49-51].
372 Although it is assumed that the colloid cantilever is smooth, the presence of nanofeatures or
373 surface heterogeneities on the colloid's surface may lead to further adhesion to the biofilm
374 surface and cause a slightly increased adhesive response. The physiochemical properties of the
375 colloid, while selected for being inert, may be modified during interaction such as the
376 attachment of EPS to the cantilever surface [52]. Although protocols were in place to ensure
377 the optimum method of measurement, EPS can attach to the cantilever surface and detach from
378 the biofilm during retraction, further use of this cantilever results in measurements between the
379 attached EPS and the biofilm causing a change in the force curve. While cleaning methods are
380 utilised to reduce the possibility of this occurring, small quantities of EPS may attach to the
381 cantilever during measurement.

382

383 4. CONCLUDING REMARKS

384

385 *P. fluorescens* biofilms resulted in higher biomass and surface coverage under semi-static, high
386 nutrient conditions. Furthermore, significant EPS production was observed. Whereas under
387 dynamic high shear conditions, low nutrient environments resulted in substantial biofilm
388 development and EPS production were observed, suggesting the introduction of dynamic
389 conditions produces a change in biofilm architecture. Further investigations into the
390 mechanical properties using AFM revealed that higher elasticity and lower adhesive properties
391 were characterised in biofilms grown under semi-static conditions and high nutrient
392 environments. The level of EPS synthesized during biofilm development is the common
393 denominator responsible for the observed biofilm phenotypes. While the analysis of
394 mechanical properties of biofilms grown under dynamic conditions was possible, it was
395 nevertheless technically challenging. Future endeavours will need to outweigh these technical
396 aspects for characterising viscoelastic biofilm properties particularly in the study of the effect
397 of shear stress. Moreover, a comprehensive understating of the relationships between the
398 growth parameters and the biofilm structure/material properties will require quantification of
399 the chemical composition of the EPS and it temporal and spatial variations.

400

401 **COMPETING INTERESTS**

402 The authors declare no conflict of interest.

403

404 **AUTHOR CONTRIBUTIONS**

405 A.A, O.H., E.C. made substantial contributions to the conception and design of the study. A.A.
406 and O.H. contributed to the acquisition and interpretation of the data. All authors participated
407 in drafting and revising the article for intellectual content.

408

409 **ACKNOWLEDGEMENTS**

410 This work was supported by the European Research Council (ERC), under grant number
411 278530 and with the financial support of Science Foundation Ireland under Grant number SFI
412 15/IA/3008. The authors thank Dr Ellen L. Lagendijk from the Institute of Biology Leiden,
413 Netherlands for the gift of the *Pseudomonas fluorescens* PCL1701 strain. We thank Prof. Suzi
414 Jarvis and the Nanoscale Function Group at UCD.

415

416 REFERENCES

- 417 [1] H.-C. Flemming, J. Wingender, The biofilm matrix, *Nature Reviews Microbiology*, 8 (2010) 623-
418 633.
- 419 [2] C. Mayer, R. Moritz, C. Kirschner, W. Borchard, R. Maibaum, J. Wingender, H.-C. Flemming, The
420 role of intermolecular interactions: studies on model systems for bacterial biofilms, *International*
421 *journal of biological macromolecules*, 26 (1999) 3-16.
- 422 [3] I. Klapper, C. Rupp, R. Cargo, B. Purvedorj, P. Stoodley, Viscoelastic fluid description of bacterial
423 biofilm material properties, *Biotechnology and Bioengineering*, 80 (2002) 289-296.
- 424 [4] A. Safari, O. Habimana, A. Allen, E. Casey, The significance of calcium ions on *Pseudomonas*
425 *fluorescens* biofilms – a structural and mechanical study, *Biofouling*, 30 (2014) 859-869.
- 426 [5] H. Cao, O. Habimana, A. Safari, R. Heffernan, Y. Dai, E. Casey, Revealing region-specific biofilm
427 viscoelastic properties by means of a micro-rheological approach, *npj Biofilms and Microbiomes*, 2
428 (2016) 5.
- 429 [6] T. Abraham, S. R. Schooling, T. J. Beveridge, J. Katsaras, Monolayer Film Behavior of
430 Lipopolysaccharide from *Pseudomonas aeruginosa* at the Air–Water Interface, *Biomacromolecules* 9,
431 no. 10 (2008): 2799-2804.
- 432 [7] J.W. Costerton, Z. Lewandowski, D.E. Caldwell, D.R. Korber, H.M. Lappin-Scott, Microbial biofilms,
433 *Annual Reviews in Microbiology*, 49 (1995) 711-745.
- 434 [8] A. Rochex, J.-M. Lebeault, Effects of nutrients on biofilm formation and detachment of a
435 *Pseudomonas putida* strain isolated from a paper machine, *Water Research*, 41 (2007) 2885-2892.
- 436 [9] B.M. Peyton, Effects of shear stress and substrate loading rate on *Pseudomonas aeruginosa*
437 biofilm thickness and density, *Water Research*, 30 (1996) 29-36.
- 438 [10] J. Moreira, L. Gomes, M. Simões, L. Melo, F. Mergulhão, The impact of material properties,
439 nutrient load and shear stress on biofouling in food industries, *Food and Bioproducts Processing*, 95
440 (2015) 228-236.
- 441 [11] W. Hu, C. Berdugo, J.J. Chalmers, The potential of hydrodynamic damage to animal cells of
442 industrial relevance: current understanding, *Cytotechnology*, 63 (2011) 445.
- 443 [12] H.J. Busscher, H.C. van der Mei, Microbial adhesion in flow displacement systems, *Clinical*
444 *Microbiology Reviews*, 19 (2006) 127-141.
- 445 [13] I.W. Sutherland, Biofilm exopolysaccharides: a strong and sticky framework, *Microbiology-Uk*,
446 147 (2001) 3-9.
- 447 [14] M.O. Pereira, M. Kuehn, S. Wuertz, T. Neu, L.F. Melo, Effect of flow regime on the architecture
448 of a *Pseudomonas fluorescens* biofilm, *Biotechnology and Bioengineering*, 78 (2002) 164-171.
- 449 [15] J.M. Moreira, L.C. Gomes, J.D. Araújo, J.M. Miranda, M. Simões, L.F. Melo, F.J. Mergulhão, The
450 effect of glucose concentration and shaking conditions on *Escherichia coli* biofilm formation in
451 microtiter plates, *Chemical Engineering Science*, 94 (2013) 192-199.
- 452 [16] H. Horn, H. Reiff, E. Morgenroth, Simulation of growth and detachment in biofilm systems under
453 defined hydrodynamic conditions, *Biotechnology and Bioengineering*, 81 (2003) 607-617.

454 [17] Y. Abe, P. Polyakov, S. Skali-Lami, G. Francius, Elasticity and physico-chemical properties during
455 drinking water biofilm formation, *Biofouling*, 27 (2011) 739-750.

456 [18] H. Hertz, Über die Berührung fester elastischer Körper, *Journal für die reine und angewandte*
457 *Mathematik*, 92 (1882) 156-171.

458 [19] A. Touhami, B. Nysten, Y.F. Dufrene, Nanoscale mapping of the elasticity of microbial cells by
459 atomic force microscopy, *Langmuir*, 19 (2003) 4539-4543.

460 [20] Y.F. Dufrêne, Sticky microbes: forces in microbial cell adhesion, *Trends in microbiology*, (2015).

461 [21] A. Méndez-Vilas, A.M. Gallardo-Moreno, M.L. González-Martín, Atomic force microscopy of
462 mechanically trapped bacterial cells, *Microscopy and Microanalysis*, 13 (2007) 55-64.

463 [22] I.B. Beech, J.R. Smith, A.A. Steele, I. Penegar, S.A. Campbell, The use of atomic force microscopy
464 for studying interactions of bacterial biofilms with surfaces, *Colloids and Surfaces B: Biointerfaces*, 23
465 (2002) 231-247.

466 [23] H.H. Fang, K.-Y. Chan, L.-C. Xu, Quantification of bacterial adhesion forces using atomic force
467 microscopy (AFM), *Journal of microbiological methods*, 40 (2000) 89-97.

468 [24] E.L. Lagendijk, S. Validov, G.E.M. Lamers, S. De Weert, G.V. Bloemberg, Genetic tools for tagging
469 Gram-negative bacteria with mCherry for visualization in vitro and in natural habitats, biofilm and
470 pathogenicity studies, *FEMS Microbiology Letters*, 305 (2010) 81-90.

471 [25] E.O. King, M.K. Ward, D.E. Raney, Two simple media for the demonstration of pyocyanin and
472 fluorescein, *The journal of laboratory and clinical medicine*, 44 (1954) 301-307.

473 [26] X. Yang, H. Beyenal, G. Harkin, Z. Lewandowski, Quantifying biofilm structure using image
474 analysis, *Journal of microbiological methods*, 39 (2000) 109-119.

475 [27] H. Beyenal, Z. Lewandowski, G. Harkin, Quantifying biofilm structure: facts and fiction,
476 *Biofouling*, 20 (2004) 1-23.

477 [28] J.L. Hutter, J. Bechhoefer, Calibration of atomic-force microscope tips, *Review of Scientific*
478 *Instruments*, 64 (1993) 1868-1873.

479 [29] P. Carl, H. Schillers, Elasticity measurement of living cells with an atomic force microscope: data
480 acquisition and processing, *Pflügers Archiv-European Journal of Physiology*, 457 (2008) 551-559.

481 [30] R. Duddu, D.L. Chopp, B. Moran, A two-dimensional continuum model of biofilm growth
482 incorporating fluid flow and shear stress based detachment, *Biotechnology and Bioengineering*, 103
483 (2009) 92-104.

484 [31] V.J. Allan, M.E. Callow, L.E. Macaskie, M. Paterson-Beedle, Effect of nutrient limitation on
485 biofilm formation and phosphatase activity of a *Citrobacter* sp, *Microbiology*, 148 (2002) 277-288.

486 [32] R. Boe-Hansen, H.-J. Albrechtsen, E. Arvin, C. Jørgensen, Bulk water phase and biofilm growth in
487 drinking water at low nutrient conditions, *Water Research*, 36 (2002) 4477-4486.

488 [33] R. Dewanti, A.C. Wong, Influence of culture conditions on biofilm formation by *Escherichia coli*
489 O157: H7, *International journal of food microbiology*, 26 (1995) 147-164.

490 [34] P. Desmond, J.P. Best, E. Morgenroth, N. Derlon, Linking composition of extracellular polymeric
491 substances (EPS) to the physical structure and hydraulic resistance of membrane biofilms, *Water*
492 *Research*, (2017).

493 [35] W.M Dunne, Bacterial adhesion: seen any good biofilms lately?, *Clinical microbiology*
494 *reviews* 15(2), (2002) 155-166.

495 [36] B.W. Peterson, H.J. Busscher, P.K. Sharma, H.C. van der Mei, Environmental and centrifugal
496 factors influencing the visco-elastic properties of oral biofilms in vitro, *Biofouling*, 28 (2012) 913-920.

497 [37] L. Vanysacker, P. Declerck, M. Bilad, I. Vankelecom, Biofouling on microfiltration membranes in
498 MBRs: role of membrane type and microbial community, *Journal of Membrane Science*, 453 (2014)
499 394-401.

500 [38] H.C. Flemming, Biofouling in water systems - cases, causes and countermeasures, *Applied*
501 *Microbiology and Biotechnology*, 59 (2002) 629-640.

502 [39] D. Nguyen, A. Joshi-Datar, F. Lepine, E. Bauerle, O. Olakanmi, K. Beer, G. McKay, R. Siehnel, J.
503 Schafhauser, Y. Wang, B.E. Britigan, Active starvation responses mediate antibiotic tolerance in
504 biofilms and nutrient-limited bacteria. *Science*, 334 (2011) 982-986.

505 [40] G. Zeng, B.S. Vad, M.S. Dueholm, G. Christiansen, M. Nilsson, T. Tolker-Nielsen, P.H. Nielsen, R.L.
506 Meyer, D.E. Otzen, Functional bacterial amyloid increases *Pseudomonas* biofilm hydrophobicity and
507 stiffness, *Frontiers in microbiology*, 6 (2014) 1099-1099.

508 [41] R. Steinberger, A. Allen, H. Hansma, P.m. Holden, Elongation correlates with nutrient
509 deprivation in *Pseudomonas aeruginosa* unsaturated biofilms, *Microbial ecology*, 43 (2002) 416-423.

510 [42] X. Li, B.E. Logan, Analysis of bacterial adhesion using a gradient force analysis method and
511 colloid probe atomic force microscopy, *Langmuir*, 20 (2004) 8817-8822.

512 [43] I.D. Auerbach, C. Sorensen, H.G. Hansma, P.A. Holden, Physical morphology and surface
513 properties of unsaturated *Pseudomonas putida* biofilms, *Journal of bacteriology*, 182 (2000) 3809-
514 3815.

515 [44] P.E. Marszalek, H. Lu, H. Li, M. Carrion-Vazquez, A.F. Oberhauser, K. Schulten, J.M. Fernandez,
516 Mechanical unfolding intermediates in titin modules, *Nature*, 402 (1999) 100-103.

517 [45] C.B. Volle, M.A. Ferguson, K.E. Aidala, E.M. Spain, M.E. Núñez, Spring constants and adhesive
518 properties of native bacterial biofilm cells measured by atomic force microscopy, *Colloids and*
519 *Surfaces B: Biointerfaces*, 67 (2008) 32-40.

520 [46] Y. Oh, N. Lee, W. Jo, W. Jung, J. Lim, Effects of substrates on biofilm formation observed by
521 atomic force microscopy, *Ultramicroscopy*, 109 (2009) 874-880.

522 [47] S. Voběrková, S. Hermanová, K. Hrubanová, V. Krzyžánek, Biofilm formation and extracellular
523 polymeric substances (EPS) production by *Bacillus subtilis* depending on nutritional conditions in the
524 presence of polyester film, *Folia microbiologica*, 61 (2016) 91-100.

525 [48] G. Francius, S. Lebeer, D. Alsteens, L. Wildling, H.J. Gruber, P. Hols, S.D. Keersmaecker, J.
526 Vanderleyden, Y.F. Dufrêne, Detection, localization, and conformational analysis of single
527 polysaccharide molecules on live bacteria, *Acs Nano*, 2 (2008) 1921-1929.

528 [49] R.J. Crawford, H.K. Webb, T. Vi Khanh, J. Hasan, E.P. Ivanova, Surface topographical factors
529 influencing bacterial attachment, *Advances in Colloid and Interface Science*, 179 (2012) 142-149.

530 [50] A. Allen, A.J.C. Semião, O. Habimana, R. Heffernan, A. Safari, E. Casey, Nanofiltration and
531 reverse osmosis surface topographical heterogeneities: Do they matter for initial bacterial
532 adhesion?, *Journal of Membrane Science*, 486 (2015) 10-20.

533 [51] M.L.B. Palacio, B. Bhushan, Bioadhesion: a review of concepts and applications, *Philosophical*
534 *Transactions of the Royal Society a-Mathematical Physical and Engineering Sciences*, 370 (2012)
535 2321-2347.

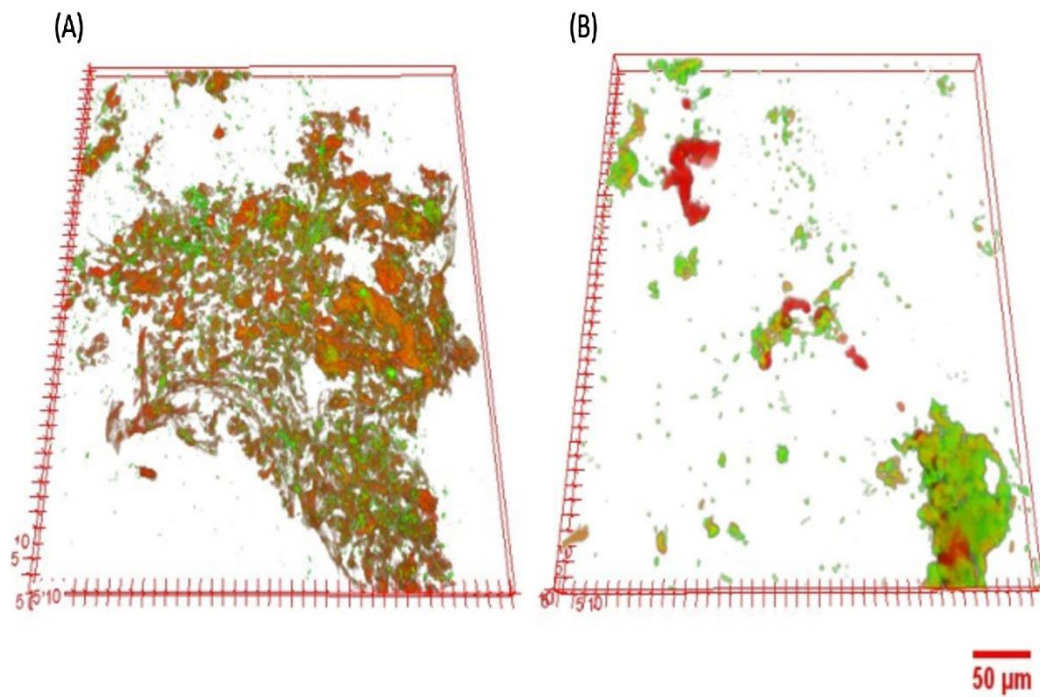
536 [52] C.B. Volle, M.A. Ferguson, K.E. Aidala, E.M. Spain, M.E. Núñez, Quantitative changes in the
537 elasticity and adhesive properties of *Escherichia coli* ZK1056 prey cells during predation by
538 *Bdellovibrio bacteriovorus* 109J, *Langmuir*, 24 (2008) 8102-8110.

539

540

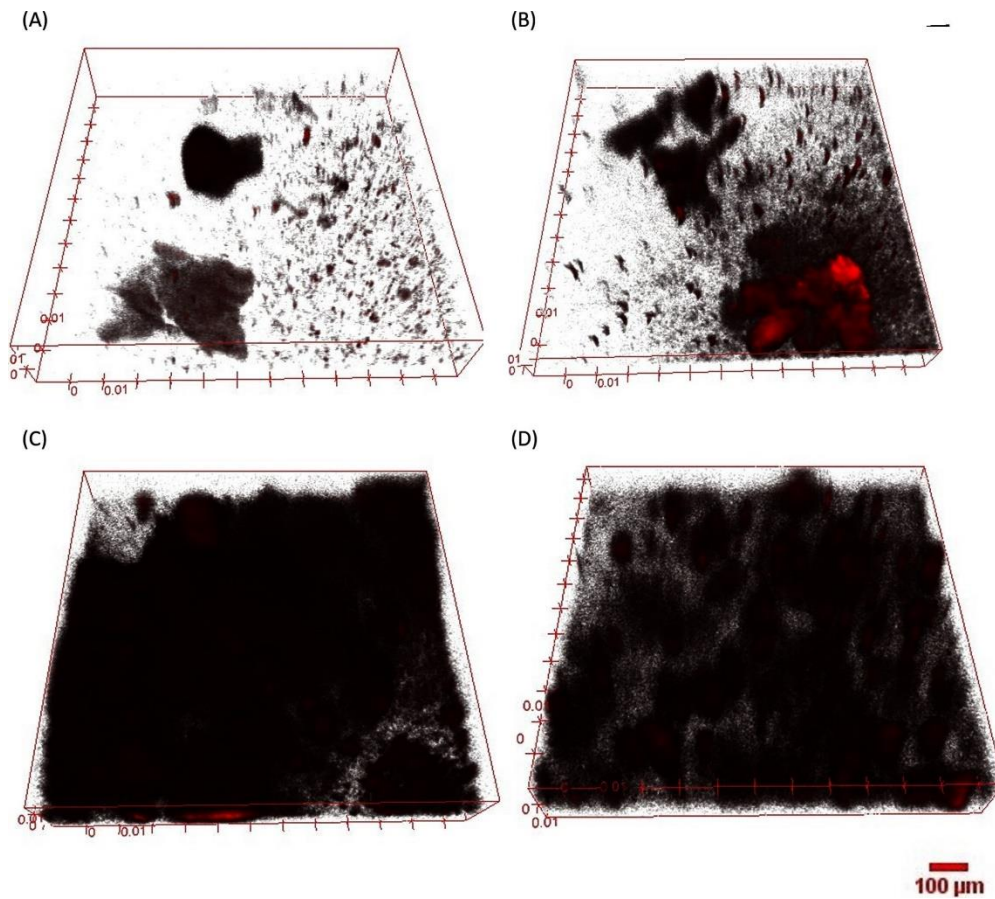
541 **Figures**

542



543

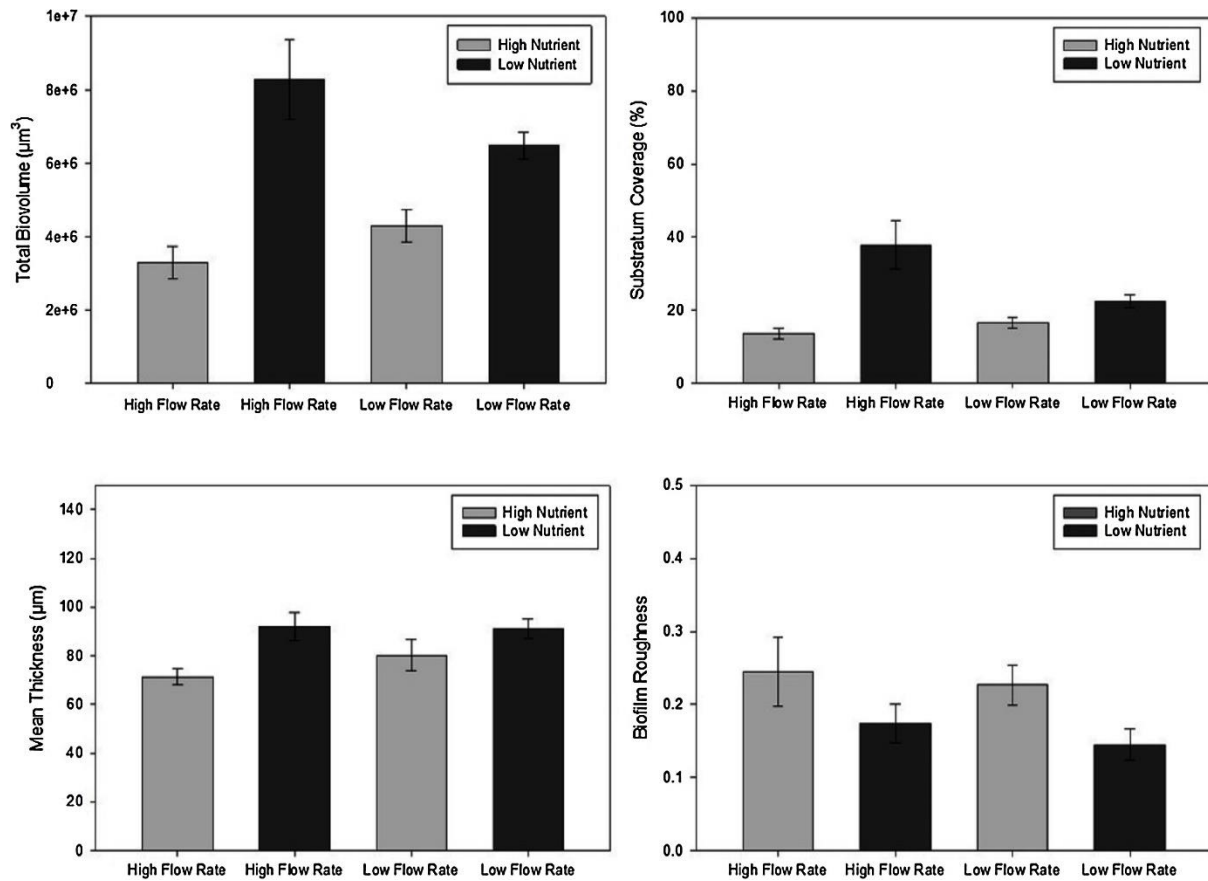
544 *Figure 1: Representative 3D reconstructed projections acquired from CLSM images of 24-*
545 *hour grown P. fluorescens under high (A) and low (B) nutrient conditions. Before microscopy,*
546 *biofilms were stained with total nucleic acid stain Syto 9[®] (green), and EPS stain ConA (red).*
547 *Three-dimensional images were created with ImageJ's "3D viewer" plugin.*



548

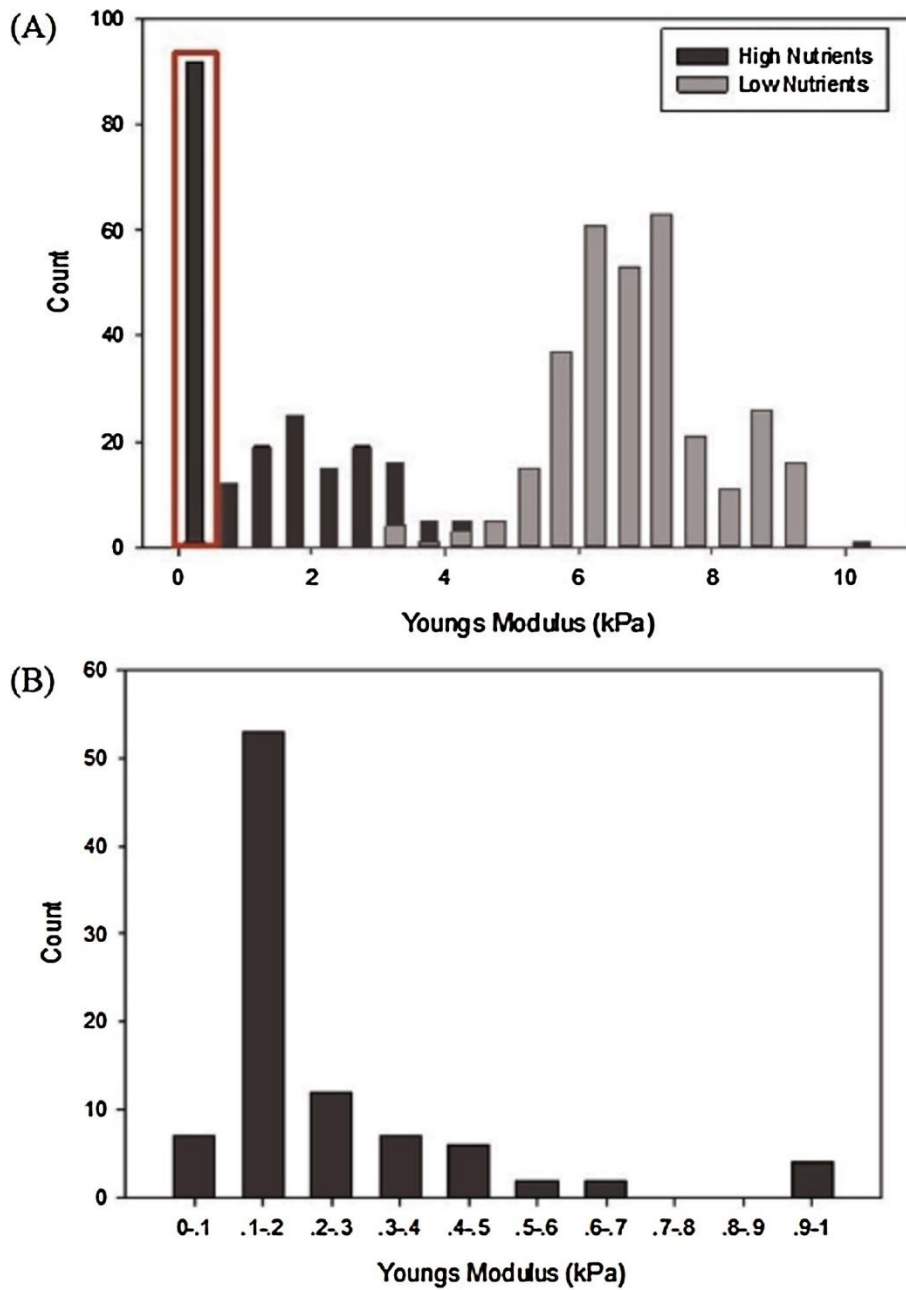
549 *Figure 2: Representative 3D reconstructed projections acquired from CLSM images of 48-*
 550 *hour mCherry expressing P. fluorescens biofilms grown in flow cells under high (A, B) and low*
 551 *(C, D) nutrient condition, under low flow rates 0.4 mL min⁻¹ (B, D) and high flow rates 0.7 mL*
 552 *min⁻¹ (A, C). Three-dimensional images were created with ImageJ's "3D viewer" plugin.*

553



554

555 *Figure 3: The structural quantification of 48-hour mCherry-expressing P. fluorescens*
 556 *biofilms, as determined by biovolume (μm^3), substratum coverage (%), mean thickness (μm)*
 557 *and biofilm roughness, following development under different nutrient (low & high) and flow*
 558 *rate (0.4 & 0.7 mL min^{-1}) conditions. Error bars represent the standard error of the shown*
 559 *average mean for each sample set.*



560

561 *Figure 4: Histogram of the Youngs Modulus (kPa) distribution of 24-hour P. fluorescens*
 562 *biofilm grown under semi-static conditions at low and high nutrient environments. (A) is the*
 563 *Youngs Modulus of high (dark grey) and low nutrients (light grey), (B) is the breakdown of the*
 564 *Youngs Modulus at high nutrients between 0 and 1 kPa as highlighted in the red section of the*
 565 *graph (A).*

566

567

568 *Table 1: Structural quantification of Syto 9[®] stained cells (total cells) and conA stained EPS*
569 *fractions following 24- hours P. fluorescens biofilm growth under semi-static conditions and*
570 *low- and high-nutrient environments. Mean values were obtained from a total of at least nine*
571 *stacks from three independent experimental runs. Error represent SE of the mean.*

		Total Biovolume [μm^3]	Substratum Coverage (%)	Mean Thickness (μm)	Biofilm Roughness
High-nutrient environment	Total cells	56988 \pm 14379	16.2 \pm 2.9	9.0 \pm 0.8	0.45 \pm 0.029
	EPS	68453 \pm 12278	20.8 \pm 3.5	10 \pm 0.7	0.46 \pm 0.053
Low-nutrient environment	Total cells	25793 \pm 4714	10.1 \pm 1.9	8.7 \pm 0.8	0.34 \pm 0.029
	EPS	18463 \pm 3129	9.30 \pm 1.9	9.10 \pm 1.2	0.35 \pm 0.027

572

573

574

575 **Table 2:** Adhesion Force and Work of Adhesion 24-hour *P. fluorescens* biofilms grown under
576 semi-static conditions at low- and high-nutrient environments. Error represent SE of the mean.

577

578

	Adhesion Force (nN)	Work of Adhesion (Aj)
High-nutrient environments	0.16 ± 0.01	5.21 ± 0.60
Low-nutrient environments	4.3 ± 0.16	185.48 ± 14.01

579

580